Cancer Research

# Novel ß-HPV49 Transgenic Mouse Model of Upper Digestive Tract Cancer

Daniele Viarisio[1], Karin Müller-Decker[1], Paola Zanna[1], Ulrich Kloz[1], Birgit Aengeneyndt[1], Rosita Accardi[2], Christa Flechtenmacher[3], Lutz Gissmann[1,4], and Massimo Tommasino[2]

## Abstract

The beta genus of human papillomaviruses (ß-HPV) includes approximately 50 different viral types that are subdivided into five species (ß-1 through ß-5). Nonmelanoma cancers may involve some ß-1 and ß-2 HPV types, but the biology of most ß-HPV types and their possible connections to human disease are still little characterized. In this study, we studied the effects of ß-3 type HPV49 in a novel transgenic (Tg) mouse model, using a cytokeratin K14 promoter to drive expression of the E6 and E7 genes from this virus in the basal skin epidermis and the mucosal epithelia of the digestive tract (K14 HPV49 E6/E7-Tg mice). Viral oncogene expression only marginally increased cellular proliferation in the epidermis of Tg animals, compared with wild-type littermates, and we observed no spontaneous tumor formation during their entire lifespan. However, we found that K14 HPV49 E6/E7-Tg mice were highly susceptible to upper digestive tract carcinogenesis upon initiation with 4-nitroquinoline 1-oxide (4NQO). This was a selective effect, as the same mice did not exhibit any skin lesions after chronic UV irradiation. Opposite results were observed in an analogous Tg model expressing the ß-2 HPV38 E6 and E7 oncogenes at the same anatomic sites. While these mice were highly susceptible to UV-induced skin carcinogenesis, as previously shown, they were little affected by 4NQO treatment. Overall, our findings highlight important differences in the biologic properties of certain ß-type HPV that affect their impact on carcinogenesis in an anatomic site-specific manner. *Cancer Res; 76(14); 4216–25. ©2016 AACR.*



## Introduction

More than 180 human papillomavirus (HPV) types have been isolated and fully sequenced. An HPV phylogenetic tree that groups the different HPV types into genera based on nucleotide sequence homology of the major capsid protein L1 has been designed (1). A subgroup of genus alpha, the high-risk (HR) HPV types, has been clearly associated with cervical cancers and a subset of oropharyngeal cancers. The transforming properties of HPV are mediated mainly by two viral oncoproteins, E6 and E7, which are able to deregulate several key cellular events, such as apoptosis and the cell cycle (2).

Genus beta comprises more than 50 HPV types and is subdivided into five different species: beta-1, -2, -3, -4, and -5 (1). In contrast to alpha HPV types, the epidemiology and biology of beta HPV types have been poorly investigated to date. Beta HPV types, namely beta-1 HPV5 and HPV8, were first isolated from individuals with an autosomal-recessive disorder termed epidermodysplasia verruciformis (3). These individuals are susceptible to infection by beta HPV types and prone to developing squamous cell carcinoma (SCC) on sun-exposed areas. More recent studies indicate that beta HPV types are also involved, together with UV radiation, in skin carcinogenesis in the normal population (3). In particular, SCC development appears to be linked mainly to HPV types within the beta-1 and beta-2 species. Accordingly, biologic studies on E6 and E7 from a few beta-1 and beta-2 HPV types (e.g., HPV8 and HPV38) have highlighted their transforming properties in *in vitro* and *in vivo* experimental models (reviewed in ref. 2).

Beta HPV types are considered to be cutaneous viruses as they are detected primarily in the skin. However, recent data have shown that they are also present in the oral mucosal epithelium, eyebrow hairs, and penile and external genital lesions (4–6). In particular, it has been shown that the beta-3 species, which includes four different HPV types (49, 75, 76, and 115) is more abundant in the nasal cavity than in the skin (7). Work from our group has shown that beta-3 HPV49 E6 and E7 have functional similarity to the mucosal HR HPV types. Coexpression of both viral oncoproteins induces immortalization of human primary keratinocytes (HPK) with a similar efficiency to HPV16 E6 and E7 (8). In addition, HPV49 E6, like E6 of the mucosal HR HPV types, mediates the interaction of the ubiquitin ligase enzyme E6AP with p53, promoting the proteasomal degradation of p53. Together, these findings suggest that beta-3 HPV49, and possibly the other three beta-3 HPV types, may also have a mucosal tropism.

To further characterize the biologic properties of HPV49 oncoproteins, in this study, we have generated a new transgenic (Tg) mouse model expressing HPV49 E6 and E7 under the control of the cytokeratin K14 promoter (9). In particular, in

[1]Deutsches Krebsforschungszentrum (DKFZ), Heidelberg, Germany. [2]International Agency for Research on Cancer (IARC), World Health Organization, Lyon, France. [3]Department of Pathology, University Hospital of Heidelberg, Heidelberg, Germany. [4]Department of Botany and Microbiology, King Saud University, Riyadh, Saudi Arabia.

**Note:** Supplementary data for this article are available at Cancer Research Online (http://cancerres.aacrjournals.org/).

**Corresponding Author:** Massimo Tommasino, Infections and Cancer Biology Group, International Agency for Research on Cancer, World Health Organization, 150 Cours A. Thomas, 69372 Lyon Cedex 08, France. Phone: 334-7273-8191; E-mail: tommasinom@iarc.fr

**doi:** 10.1158/0008-5472.CAN-16-0370





AACR

this *in vivo* model we have compared the ability of HPV49 E6 and E7 to cooperate with different carcinogens and have further highlighted some functional similarities to E6 and E7 of the mucosal HR HPV types.

## Materials and Methods

### Plasmid construction, generation, and characterization of Tg mice

The generation of HPV16 and HPV49 E6 and E7 plasmids and Tg mouse lines was performed following the procedures described previously (10). One line was generated for FVB/N K14 HPV16 E6/E7-Tg mice and three lines for FVB/N K14 HPV49 E6/E7-Tg mice. FVB/N K14 HPV38 E6/E7-Tg mice have been previously described and characterized (10). All experiments described in this study were performed in strict accordance with federal law and standard ethical guidelines (11, 12) and approved by local government authorities (Regierungspräsidium, Karlsruhe, Germany) under licenses G162-08, G164-12, and G35-13. UV irradiation was performed under sevoflurane anesthesia, and every effort was made to minimize suffering. Determination of viral genome copy number, quantification of E6/E7 mRNA levels, and histologic and immunohistochemical analysis were performed as described in Supplementary Materials and Methods and primers listed in Supplementary Table S1.

### UV treatment

UVB irradiation was performed following the procedures and protocols described previously (10). Experimental animal groups included 7-week-old female: (i) FVB/N WT ($n = 30$); (ii) K14 HPV38 line 187 ($n = 30$); (iii) HPV49 line 3 ($n = 21$). Tumors were identified first macroscopically and then by histologic diagnosis.

### Initiation–promotion experiments

All experiments were performed following the procedures described previously (10). Experimental animal groups included 7-week-old female: (i) FVB/N WT ($n = 43$); (ii) K14 HPV38 line 187 ($n = 27$); (iii) HPV49 line 3 ($n = 29$); (iv) HPV49 line 2 ($n = 9$). Tumors were identified first macroscopically and then by histologic diagnosis.

### 4NQO treatment

Experimental groups of 6-week-old female WT ($n = 20$) mice or K14 HPV E6/E7-Tg mice of HPV type 38 ($n = 5$), 49 ($n = 5$), or 16 ($n = 5$) were given water with 1% of 1,2-propylene glycol (PPG) in tap water as control, and cohorts of WT mice ($n = 28$) or K14 HPV E6/E7-Tg mice of HPV type 38 ($n = 18$), 49 ($n = 15$), or 16 ($n = 14$) were given water with the carcinogen 4NQO (10 μg/mL drinking water containing 1% PPG vehicle) for 16 weeks and then received normal water again. The drinking water batches were exchanged every week to ensure no degradation of the carcinogen. The daily consumption of water, adjusted for the initial weight of the animals, was $4.8 \pm 0.4$ mL per mouse. No significant difference in water consumption was observed among the four groups of animals. Body weight was measured weekly. If the body weight was decreased by $\geq$20% relative to the maximum weight, the mouse was killed and analyzed for the presence of tumors in the oral cavity or the digestive tract. When a tumor was found in one of the three listed anatomic regions (tongue, esophagus, forestomach), the incidence was recorded. Sections of lesions were then taken and snap-frozen in liquid nitrogen or embedded in paraffin for histologic analysis.

### Transcriptome analysis

Experimental groups of 7-week-old WT ($n = 9$) mice or K14 HPV38 line 187 ($n = 8$) or HPV49 line 3 ($n = 6$) Tg mice were shaved and irradiated 5 times in 5 consecutive days with a UVB dose of 450 mJ/cm$^2$. Age- and sex-matched groups of WT ($n = 8$) mice or K14 HPV38 line 187 ($n = 7$) or HPV49 line 3 ($n = 6$) Tg mice were taken as untreated control. At 1 hours after the last UVB irradiation, the mice were killed and the skin removed and quickly frozen. Keratinocytes were subsequently isolated via mechanical abrasion and snap frozen in liquid nitrogen.

Transcriptome analysis was performed on an Illumina system using mouseWG-6 v2 BeadChip (Illumina) in two different experiments. The data were normalized using Chipster (13). After quality assessment, only the transcripts that showed a SD lower than 0.9 were used for the analysis and only differences that were significant with $P < 0.05$ in a two-group test were then considered. Pathway analysis was done using the functional annotation tool of DAVID Bioinformatics Resources 6.7 (14, 15; $P$ value < 0.01, FDR < 0.05, and fold of enrichment > 2).

### Statistical analysis

Time to first tumor and time to SCC were displayed with Kaplan–Meier plots. Time to first tumor and time to SCC were compared between the different groups with the log-rank test. Statistical analyses were performed with SigmaPlot (version 12.5, copyright 2015, Systat Software Inc).

## Results

### Generation and characterization of K14 HPV49 E6/E7-Tg mice

To further characterize the biologic properties of HPV49 E6 and E7 oncoproteins, we generated Tg mouse lines expressing the two viral oncogenes under the control of the human K14 promoter, which is active in the basal layer of the epidermis (9), the putative HPV infection site. The construct shown in Fig. 1A was microinjected into the pronuclei of fertilized eggs and, after birth, transgene-positive offspring were identified by PCR using as a template DNA extracted from tail biopsies and specific primers for the HPV49 E6/E7 construct. Three independent Tg mouse lines (lines 1–3) were identified and bred successfully. We first determined by quantitative RT-PCR (qRT-PCR) the expression of the viral genes in the epithelium of different anatomic sites in the three Tg lines. A similar pattern of the viral gene expression was observed in the three Tg lines (Fig. 1B). In addition, the viral mRNA levels were considerably lower in the ear compared with the other three anatomic sites (Fig. 1B).

Hematoxylin and eosin (H&E)-stained sections of dorsal skin, ear, tongue, and esophagus did not reveal any significant morphologic alterations in the epithelia of K14 HPV49 E6/E7-Tg mice (line 3) compared with wild-type (WT) mice (Fig. 2A). In addition, immunohistochemical staining for Ki67 revealed that the viral oncoproteins only slightly increased the proliferation of basal layer keratinocytes in the tongue and the esophagus, while no significant effect was observed in the dorsal skin or ear epidermis (Fig. 2B). Similar data were obtained with Tg animals of older age and line 2 (data not shown). In

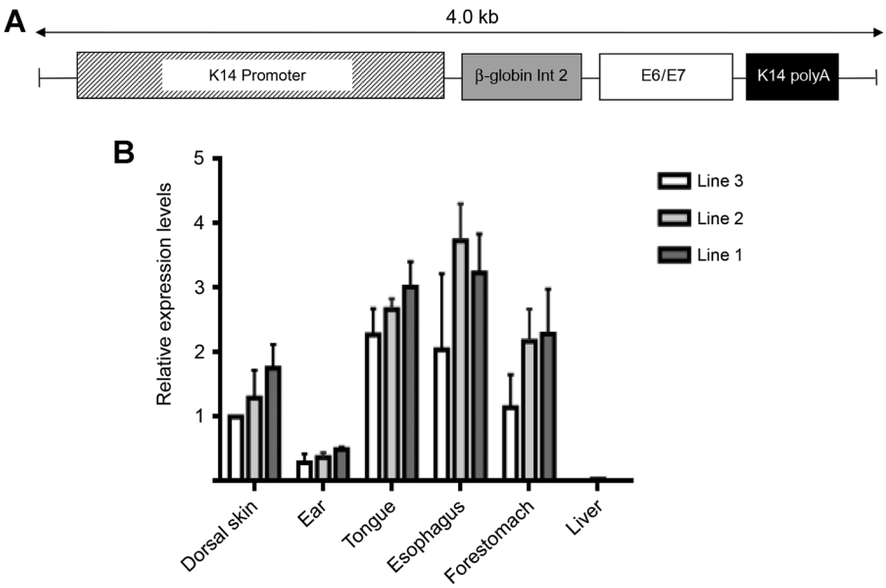


**Figure 1.**
HPV49 E6 and E7 expression in Tg mice. A, schematic representation of the K14 HPV49 E6/E7 construct. B, HPV49 E6 and E7 transcripts are similarly expressed in the epithelia of the three hemizygous Tg mouse lines 1, 2, and 3. Total RNA was extracted from the dorsal skin, ear, tongue, esophagus, forestomach, and liver of the three lines. After preparation of cDNA, E6 and E7 expression was determined by qRT-PCR and normalized to the expression level of keratin 14. The data shown in the figures refer to E7 expression and are the means ± SEM of three independent experiments. In each experiment, the data for dorsal skin line 3 were set to 1 and the other values consequently resized.

addition, the K14 HPV49 E6/E7-Tg mice did not spontaneously develop any type of lesion during their life span.

### WT and K14 HPV49 E6/E7-Tg mice show similar susceptibility to skin SCC development after DMBA/TPA treatment

Previous studies from our group reported that beta-2 HPV38 E6 and E7 expression under the control of the K14 promoter significantly increased the incidence of papillomas and SCC in the skin of Tg animals exposed to chemical carcinogens (10). Therefore, we compared the tumor susceptibility of WT mice, K14 HPV38 E6/E7-Tg mice, and K14 HPV49 E6/E7-Tg mice in the multistage skin carcinogenesis protocol using 7,12-dimethylbenz[*a*]anthracene (DMBA) as initiator and 12-*O*-tetradecanoylphorbol-13-acetate (TPA) as tumor

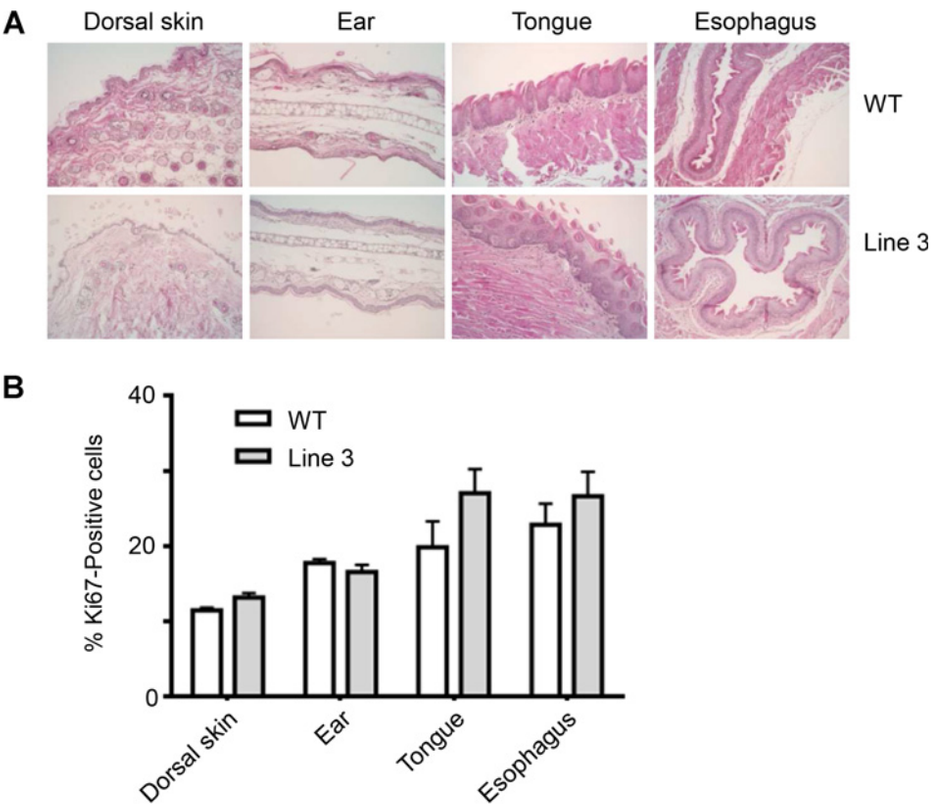


**Figure 2.**
Histologic analysis of epithelial specimens from WT and K14 HPV49 E6/E7-Tg mice of line 3. A, representative images (original magnification, ×40) of H&E-stained paraffin sections of dorsal skin, ear, tongue, and esophagus. B, analysis of cellular proliferation in the epithelia of WT and Tg mice. Quantification of Ki67-positive cells in WT and Tg epithelia was done by counting 400 hematoxylin-stained cells under ×40 magnification in four different fields of different epithelia of $n = 4$ mice/group. Ki67 quantification differences between wild-type and Tg animals were not significant as determined by *t*-test analysis: dorsal skin, Tg versus WT, $P = 0.0602$; ear, Tg versus WT, $P = 0.3195$; tongue, Tg versus WT, $P = 0.1781$; esophagus, Tg versus WT, $P = 0.4091$.

promoter. All animals were exposed to a single DMBA treatment followed by repeated TPA treatments for 20 weeks and subsequent monitoring for a further 10 weeks (10). In agreement with our previous data, K14 HPV38 E6/E7-Tg animals developed papillomas and SCC much faster and in larger numbers compared with the WT animals (Fig. 3A–D). Only 5 HPV49 E6/E7-Tg animals (line 3), out of 29, developed a single lesion each 5 weeks earlier than the rest of the WT group (Fig. 3A). However, no significant difference was observed between the two groups of animals in the average number of tumors per animal or the number of mice bearing SCC (Fig. 3B–D). The difference between WT and HPV49 E6/E7-Tg animals was even less evident with another line of Tg animals (line 2; Supplementary Fig. S1). The control groups, treated with the vehicle alone (acetone), did not develop any lesion during the experimental and observation time (data not shown).

### E6 and E7 of HPV38 and HPV49 cooperate differently with UV irradiation in promoting skin lesions and with 4NQO in promoting upper digestive tract lesions

UV irradiation is a key risk factor for nonmelanoma skin cancer (NMSC) in humans. We previously showed that although K14 HPV38 E6/E7-Tg mice did not spontaneously develop any tumors during their life span, they were highly susceptible to UV-induced skin carcinogenesis (10). Exposure of HPV38 E6/E7-Tg mice to chronic UV irradiation resulted in the development of actinic keratosis–like lesions, considered to

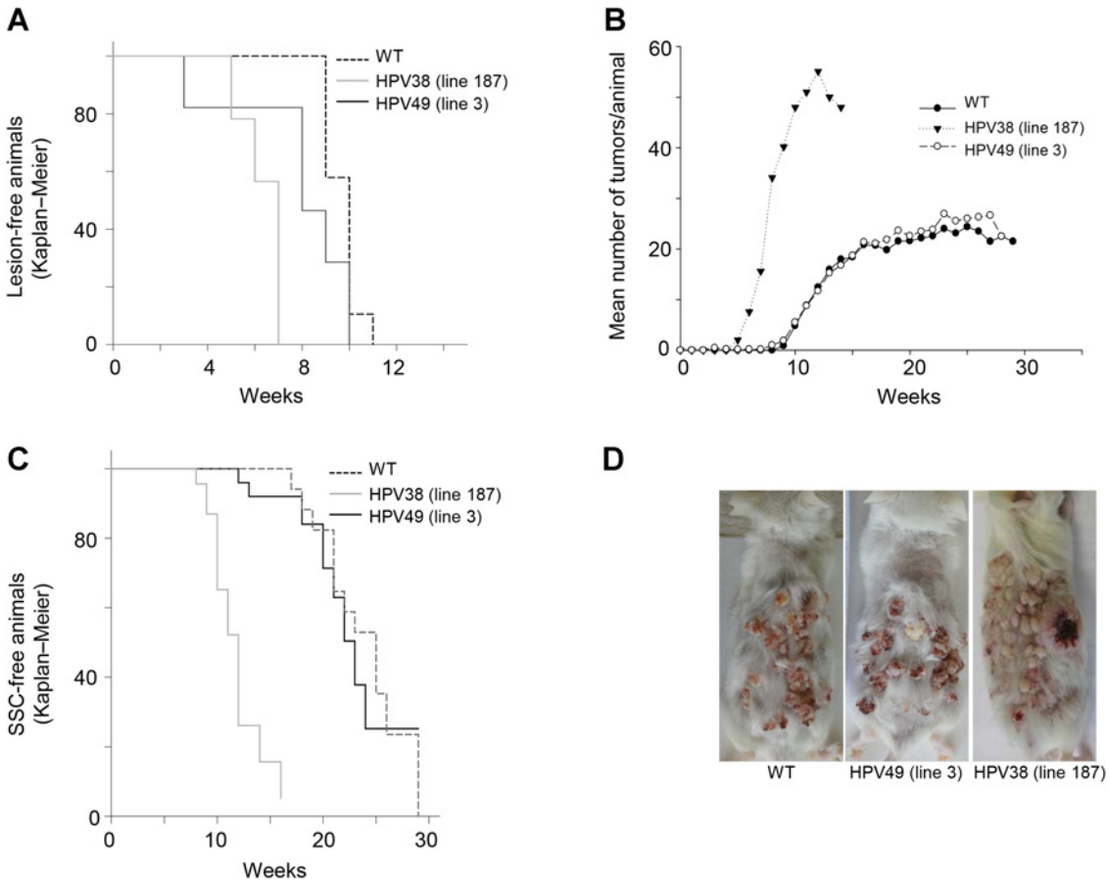


**Figure 3.**

Tumor burden in WT and HPV E6/E7-Tg mouse lines of HPV types 38 line 187 and 49 line 3 after DMBA/TPA treatment. A, skin lesion-free animals. Kaplan–Meier analysis of animals with skin tumors in WT and Tg cohorts. Experimental groups of 7-week-old female FVB/N WT ($n = 33$), HPV38 E6/E7-Tg line 187 ($n = 27$), or K14 HPV49 E6/E7-Tg line 3 ($n = 29$) mice were exposed to DMBA/TPA standard treatment. Skin tumor formation was recorded weekly until week 30 after the start of tumor promotion by TPA. The following differences between animal groups were significant: K14 HPV49 E6/E7-Tg versus WT, $P < 0.001$; K14 HPV49 E6/E7-Tg versus K14 HPV38 E6/E7–Tg, $P < 0.001$; K14 HPV38 E6/E7-Tg versus WT, $P < 0.001$, as determined by the log-rank test for group data. B, tumor multiplicity. Average number of tumors per animal in FVB/N WT and Tg cohorts. As of week 6, the number of tumors/animal developed by the K14 HPV38 E6/E7-Tg mice was significantly higher compared with K14 HPV49 E6/E7-Tg mice or WT mice: $P < 0.05$ ($P < 0.001$ as of week 7) as determined by the two-group *t*-test analysis. The difference in the number of tumors/animal between K14 HPV49 E6/E7-Tg mice and WT mice was not significant in any time point of the experiment. C, cutaneous SCC-free animals. Kaplan–Meier analysis of animals with skin SCC in WT and Tg cohorts. SCC development was confirmed by histologic analyses. The difference between the curves of K14 HPV38 E6/E7-Tg mice and WT or K14 HPV49 E6/E7-Tg mice is statistically significant ($P < 0.001$, as determined by the log-rank test for group data). The difference between the curves of WT and K14 HPV49E6/E7-Tg mice is not statistically significant ($P = 0.807$). D, representative images of dorsal skin from WT and HPV E6/E7-Tg mouse lines 12 weeks after the start of tumor promotion by TPA.

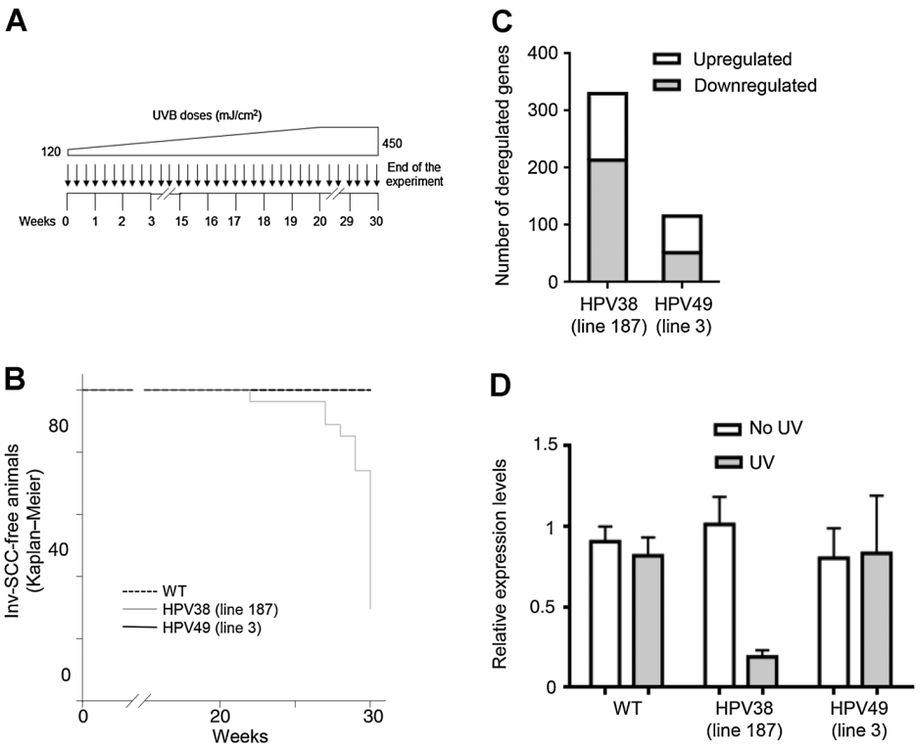


**Figure 4.**

Tumor burden in WT and HPV E6/E7-Tg mouse lines after UVB irradiation. A, groups of 7-week-old female K14 HPV49 E6/E7-Tg line 3 mice ($n = 21$), K14 HPV38 E6/E7-Tg line 187 mice ($n = 30$), and FVB/N WT mice ($n = 30$) were long-term UVB irradiated as schematically shown in the diagram. B, cutaneous SCC-UVB–induced free animals. Kaplan–Meier analysis of animals with skin SCC in WT and Tg group. The difference between the curves of K14 HPV38 E6/E7-Tg mice and WT or K14 HPV49 E6/E7-Tg mice is statistically significant ($P < 0.001$, as determined by the log-rank test for group data). C, cellular gene expression profile in the skin of WT and Tg animals upon UV irradiation. The number of genes differentially regulated (up- or downregulated) in the skin of HPV38 or 49 Tg mice versus WT mice upon UV irradiation is indicated in the histogram. D, quantification of IL18 mRNA levels induced by UV irradiation in WT and Tg animals. The IL18 mRNA levels were determined by RT-PCR. The values are obtained by the analysis of total RNA extracted from four different animals for each group. The differences in IL18 mRNA expression between UVB-irradiated K14 HPV38 E6/E-Tg mice and all the other groups are statistically significant ($P < 0.05$, as determined by two-group *t*-test analysis).

be precursors of SCC in humans, and subsequently of SCC. In contrast, WT animals subjected to identical treatment did not develop any type of skin lesions. On the basis of these results, we next determined whether HPV49 E6 and E7 can synergize with UV irradiation to promote skin lesions. Tg animals were UV irradiated for 30 weeks as described previously (Fig. 4A; ref. 10). Again, results for the K14 HPV49 E6/E7-Tg mice were similar to those for the WT animals, and the mice did not develop any type of skin lesions during the chronic treatment (Fig. 4B). In contrast, the majority of K14 HPV38 E6/E7-Tg mice developed premalignant skin lesions and SCC (Fig. 4B).

To gain further mechanistic insights into the different behavior of K14 HPV38 E6/E7 and K14 HPV49 E6/E7-Tg mice after UV irradiation, we analyzed the entire transcriptome profile in the skin of WT and Tg mice exposed or nonexposed to UV irradiation. We analyzed the gene expression changes induced by UV irradiation in the two Tg mice models compared with the WT animals. As shown in Fig. 4C, in UV-irradiated K14 HPV38 E6/E7-Tg mice, approximately 300 cellular genes were deregulated compared with the WT animals exposed to the same treatment. In contrast, this phenomenon was much attenuated in K14 HPV49 E6/E7-Tg mice (Fig. 4C). The pathway enrichment analysis revealed that specific cellular pathways are exclusively targeted by HPV38, but not HPV49, for example, some members of the IL1 family pathway (Supplementary Table S2). In particular, our initial validation studies revealed that the expression of IL18 is inhibited in UV-irradiated HPV38 E6/E7-Tg mice, in contrast to WT and HPV49 E6/E7-Tg mice, which expressed high levels of IL18 mRNA in the skin after UV irradiation (Fig. 4D).

It has been shown that the K14 promoter–driven expression of E6 and E7 from the mucosal HR HPV type 16 in the basal layer of mouse epithelia strongly cooperates with the chemical carcinogen 4-nitroquinoline 1-oxide (4NQO) in promoting head and neck SCC when given continuously in drinking water (16). 4NQO causes a broad spectrum of DNA damage similar to that induced by tobacco-associated carcinogens (17–21).

On the basis of our data obtained in *in vitro* experimental models that revealed functional similarities between beta-3 HPV49 and mucosal HR HPV16 (1), we investigated whether K14 HPV49 E6/E7-Tg mice have an altered susceptibility to 4NQO-induced carcinogenesis compared with WT animals. A group of K14 HPV16 E6/E7-Tg mice was included in the experiment as a positive control, together with a group of K14 HPV38 E6/E7-Tg mice representing the beta-2 genus. Mice were exposed to 4NQO continuously via the drinking water for

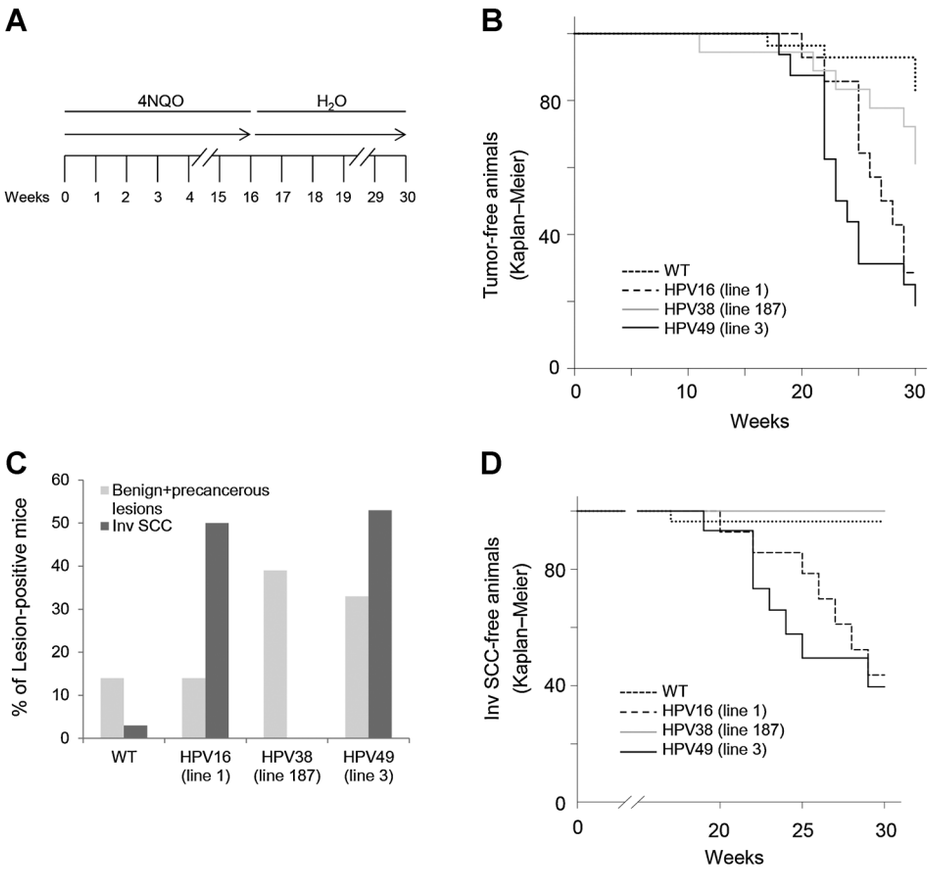


**Figure 5.**
Tumor burden in WT and HPV E6/E7-Tg animal lines after 4NQO treatment. A, WT mice ($n = 28$) or K14 HPV E6/E7-Tg mice of HPV type 38 ($n = 18$), 49 ($n = 15$), or 16 ($n = 14$) were exposed to 4NQO treatment as schematically shown in the diagram. B, tumor-free animals. Kaplan–Meier analysis of animals with tumors in the oral cavity or digestive tract. Benign, precancerous, and invasive lesions were considered. The following differences between animal groups were significant: K14 HPV49 E6/E7-Tg versus WT, $P < 0.001$; K14 HPV49 E6/E7-Tg versus K14 HPV38 E6/E7–Tg, $P < 0.05$; K14 HPV16 E6/E7-Tg versus WT, $P < 0.001$, as determined by the log-rank test for group data. The following differences between animal groups were not significant: K14 HPV16 E6/E7-Tg versus K14 HPV38 E6/E7-Tg, $P = 0.165$; K14 HPV38 E6/E7-Tg versus WT, $P = 0.181$; K14 HPV16 E6/E7-Tg versus K14 HPV49 E6/E7-Tg, $P = 0.229$, as determined by the log-rank test for group data. C, percentage of animals in WT and Tg cohorts bearing benign and precancerous lesions or at least one invasive SCC. D, invasive SCC-free animals. Kaplan–Meier analysis of animals bearing SCC. Upon histologic analysis, the mice with at least one SCC in the oral cavity or upper digestive tract were counted as positive. The following differences between animal groups were significant: K14 HPV49 E6/E7-Tg versus WT, $P < 0.001$; K14 HPV49 E6/E7-Tg versus K14 HPV38 E6/E7-Tg, $P < 0.001$; K14 HPV16 E6/E7-Tg versus WT, $P < 0.005$; K14 HPV16 E6/E7-Tg versus K14 HPV38 E6/E7–Tg, $P < 0.005$, as determined by the log-rank test for group data. The following differences between animal groups were not significant: K14 HPV38 E6/E7-Tg versus WT $P = 0.682$; K14 HPV16 E6/E7-Tg versus K14 HPV49 E6/E7-Tg, $P = 0.502$, as determined by the log-rank test for group data.

16 weeks (Fig. 5A). Animals then received normal water again and were followed up for an additional 14 weeks, with their body weight monitored weekly. Animals that showed $\geq$20% loss of body weight relative to their maximum weight or that looked sick were killed to determine the presence of possible lesions in the oral cavity and/or the upper digestive tract, including the tongue, esophagus, forestomach, and stomach. In K14 HPV49 E6/E7-Tg mice, HPV49 E6 and E7 strongly synergized with 4NQO in the induction of tumors at these anatomic sites (Figs. 5 and 6; Table 1). Similar survival curves were observed for K14 HPV49 E6/E7-Tg and K14 HPV16 E6/E7-Tg mice, translating into similar tumor-free animals curves (Fig. 5B). In contrast, WT and K14 HPV38 E6/E7-Tg mice showed a much lower susceptibility to 4NQO-driven carcinogenesis (Fig. 5B). No strong differences were detected for HPV genome copy number and E6/E7 transcript levels among the three Tg models (Supplementary Fig. S2), indicating that the results obtained in the different Tg models are not due to a high difference in the expression levels of viral transcripts.

Necropsies from the tongue, palate, esophagus, and forestomach were systematically collected and histopathologically analyzed. The results of this diagnosis are presented in Table 1. The percentage of mice found to be positive for benign and precancerous lesions or invasive SCC is shown in Fig. 5C, and the Kaplan–Meier curve for SCC-free animals is shown in Fig. 5D. Only one mouse in the WT group developed an invasive SCC, and only *in situ* carcinoma–like lesions, also called papillomas, characterized by high nuclear atypia, were detected in K14 HPV38 E6/E7-Tg mice. HPV49 E6/E7-Tg mice appeared to be even more sensitive to 4NQO-induced carcinogenesis

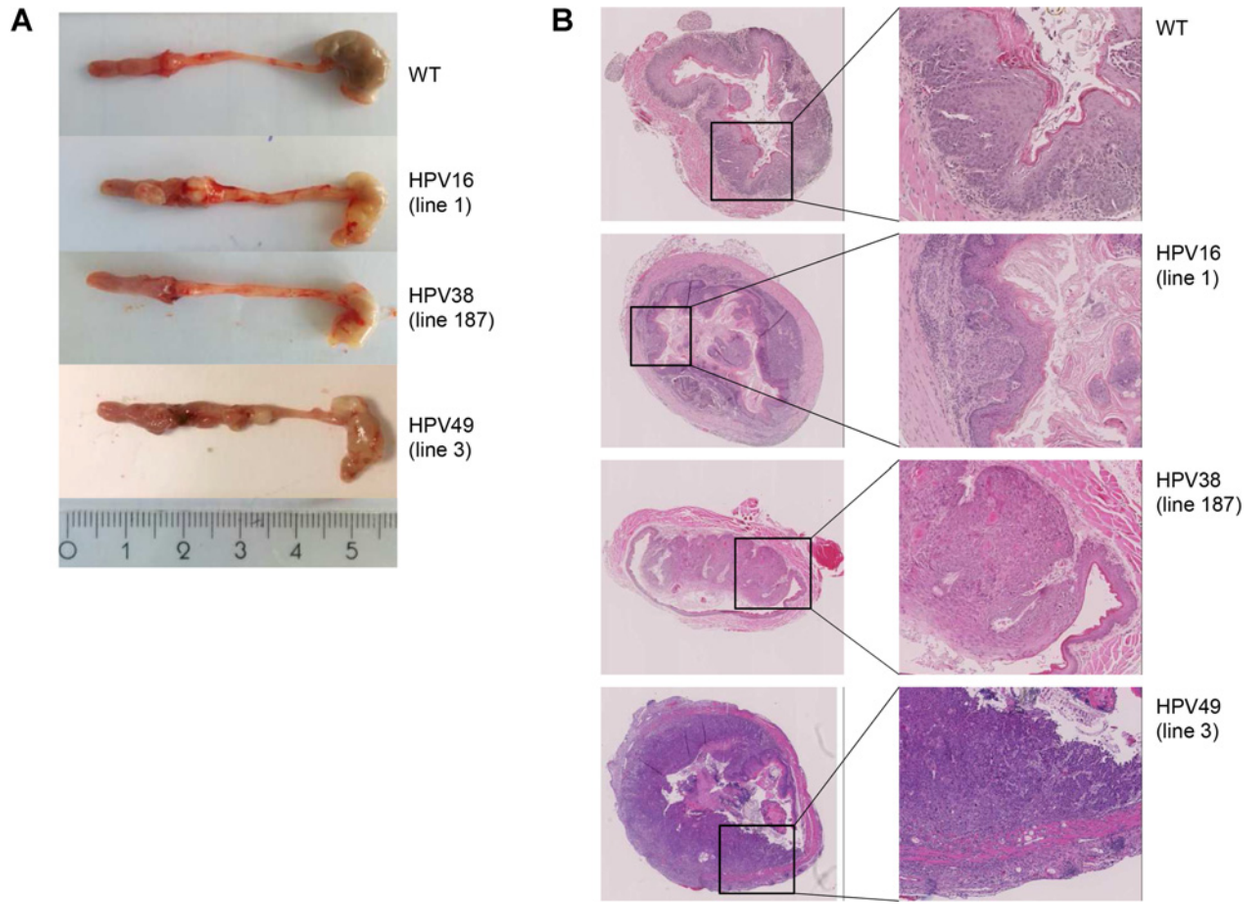


**Figure 6.**

4NQO-induced lesions. A, representative images of tongue and upper digestive tract isolated from WT or Tg mice that developed lesions after 4NQO treatment. From top to bottom, WT organs with no lesions, K14 HPV16 E6/E7-Tg organs with SCC in the esophagus, K14 HPV38 E6/E7-Tg organs with papillomas plus atypia in the esophagus, and K14 HPV49 E6/E7-Tg organs with SCC on the tongue and in the esophagus. B, representative images of H&E-stained sections from WT or Tg mice that developed lesions after 4NQO treatment. From top to bottom, section of esophagus from a WT mouse, section of esophagus from a K14 HPV16 E6/E7-Tg mouse, section of esophagus from a K14 HPV38 E6/E7-Tg mouse, and section of esophagus from a K14 HPV49 E6/E7-Tg mouse (original magnification, ×5). Magnified areas are shown in the right panels.

than HPV16 E6/E7-Tg mice, showing the highest number of benign lesions and SCC of the four groups of animals (Table 1; Fig. 5C). In addition, the development of invasive SCC appeared to be slightly accelerated in HPV49 E6/E7-Tg mice compared with HPV16 E6/E7-Tg mice (Fig. 5D).

A small number of the most representative lesions for the four groups of animals are shown in Fig. 6A and B. The esophagus section of a WT mouse presented light to medium dysplasia with enlarged and irregular nuclei in the basal layer and numerous mitosis (Fig. 6B, WT). The esophagus section of a K14 HPV16 E6/E7-Tg mouse showed diffuse SCC clearly invading the submucosa, characterized by a small area of keratinization and accompanying inflammatory cells (Fig. 6B, HPV16, line 1). The esophagus section of a K14 HPV38 E6/E7-Tg mouse displayed *in situ* carcinoma with atypical cells distributed diffusely throughout all epithelial layers, numerous mitosis, and areas of keratinization, but showed no invasiveness (Fig. 6B, HPV38, line 187). The esophagus section of a K14 HPV49 E6/E7-Tg mouse showed a SCC with atypical squamous epithelial cells broadly infiltrating the underlying muscular fibers (Fig. 6B, HPV49, line 3).

## Discussion

Genus beta HPV types form a large group in the HPV phylogenetic tree and are subdivided into five species. On the basis of biologic and epidemiologic data, some HPV types within the beta-1 and beta-2 species are likely to be involved, together with UV irradiation, in the development of NMSC (2, 3, 22). However, very little is known about the biology of most beta HPV types and whether they are linked to additional human diseases. Recent studies have reported that DNA of beta HPV types can be detected at different anatomic sites (4–6, 23, 24). In particular, the beta-3 HPV types appear to be more abundant in the nasal cavity than in the skin (24). Experiments performed in HPKs, the natural host of HPV, highlighted some functional similarities between mucosal HR HPV types such as HPV16 and beta-3 HPV49 (8). Indeed, HPV49

**Table 1.** Analysis of tumors in WT and Tg animal lines. After the animals were killed, necropsies from the oral cavity (tongue) and upper digestive tract (esophagus and forestomach) were collected, and histologic diagnosis was performed, which included classification and staging of tumors into benign and precancerous lesions versus malignant lesions

| Mouse strain | Number of mice | Positive-tumor mice (%) | Positive-tumor organ | Diagnosis (number) |
|---|---|---|---|---|
| WT | 28 | 5 (18) | Tongue | Papilloma (1)<br>SCC (1) |
| | | | Esophagus | Light dysplasia (3) |
| HPV38 Tg | 18 | 7 (8) | Tongue | Papilloma (1) |
| | | | Esophagus | Parakeratosis (1)<br>Papilloma with atypia (5) |
| HPV49 Tg | 15 | 13 (87)[a] | Tongue | Papilloma (2)<br>Papilloma with atypia (2)<br>SCC (7) |
| | | | Esophagus | Papilloma (4)<br>Papilloma with atypia (5)<br>SCC (4)[b] |
| HPV16 Tg | 14 | 9 (64)[a] | Tongue | Papilloma with atypia (1)<br>SCC (1) |
| | | | Esophagus | Papilloma (1)<br>Papilloma with atypia (2)<br>SCC (4) |
| | | | Forestomach | SCC (4)[b] |

[a]Mice had lesions in more than one organ.
[b]The majority of the SCC is invasive.

E6 is able to induce p53 degradation via the interaction with ubiquitin ligase enzyme E6AP, as previously shown for the mucosal HR HPV types. Sequence alignments show that a number of HPV16 E6 residues that are critical for E6AP peptide and p53 binding are conserved in HPV49 E6, but not in HPV38 E6. We found that Arg55 and Arg131 of HPV16 E6, which provide crucial contacts to acidic residues of the LxxLL peptide of E6AP (25), are conserved (at least as positively charged residues) in HPV49 E6, but not in HPV38 E6. Similarly, the key p53-binding residue Asp49 (26) is conserved in HPV49, whereas it becomes an Asn residue in HPV38 E6 (Supplementary Fig. S3). Thus, taking into consideration these experimental and epidemiologic observations, it is likely that the beta-3 species are able to colonize the mucosal epithelia.

In this study, we showed that in Tg mouse models, HPV49 E6 and E7 oncoproteins strongly synergize with 4NQO, a carcinogen widely used in *in vivo* experimental models for oral cavity carcinogenesis (27). In a similar study challenging the HR HPV16 E6/E7-Tg mouse model with the same 4NQO concentration it was found that the mucosal HR HPV16 E6 and E7 oncoproteins considerably increased 4NQO carcinogenicity in the oral cavity (16). In our experiments performed in Tg animals, we observed that HPV49 E6 and E7 had an efficiency similar to, or higher than, that of HPV16 E6 and E7 in synergizing with 4NQO. Importantly, HPV49 E6 and E7 did not increase the susceptibility of the Tg mice to UV-induced carcinogenesis in the skin. An opposite scenario was observed in HPV38 E6/E7-Tg mice, which showed high susceptibility to UV irradiation and low susceptibility to 4NQO-induced carcinogenesis. Thus, in Tg mouse models, E6 and E7 from HPV38 and HPV49 have the ability to synergize with different carcinogens at different anatomic sites. These findings highlight fundamental differences in the biologic properties of the two virus types and further support the hypothesis that they may have a different tropism. These findings also suggest that HPV49 could promote, together with additional environmental factors, the development of malignant lesions in the upper digestive tract or other anatomic sites. Although it has been reported that beta HPV types are abundantly present in the oral cavity (4–6), no data are available for their distribution in other sites of the digestive tract. In addition, no epidemiologic studies have evaluated the possible presence of any beta HPV types in cancerous tissue of the digestive tract. Thus, additional studies are required to evaluate the possible involvement of beta-3 HPV types in human carcinogenesis.

Cells of mucosal or cutaneous epithelia are exposed to different types of DNA-damaging agents, leading to activation of cellular responses that induce cell-cycle arrest or apoptosis to allow, respectively, repair or elimination of the damaged cell. As all HPV types rely on the DNA replication machinery of the infected cell, they have developed several mechanisms to promote cellular proliferation and efficiently replicate their own DNA even in the presence of cellular stress. For instance, the cutaneous beta HPV types, to guarantee the replication of their own DNA, must be able to circumvent the adverse effect of UV irradiation on keratinocyte proliferation. Indeed, many studies have shown that some beta HPV types are able to efficiently circumvent the antiproliferative effects of UV irradiation (reviewed in ref. 2), facilitating the accumulation of UV-induced DNA mutations (28, 29). The fact that HPV49 E6 and E7 are not able to stimulate UV-induced skin carcinogenesis in the Tg mouse model suggests that this virus has not developed mechanisms to overcome the cellular stress due to UV irradiation. In agreement with this hypothesis, we have observed that E6 and E7 from HPV38 and HPV49 showed substantial differences in deregulating the cellular gene expression patterns induced by UV irradiation. In particular, our initial data show that HPV38 E6 and E7, by altering cellular gene expression, strongly inhibit the inflammasome activation induced by UV irradiation, whereas HPV49 E6 and E7 do not have any effect on this activation. Interestingly, an independent study provided evidence that the inflammasome activation induced by UV irradiation is involved in the repair of DNA damage and in UVB-induced apoptosis (30, 31). Thus, the lack of synergism between HPV49 oncoproteins and UV irradiation in skin carcinogenesis may be explained by their inability to target the UV-induced inflammasome. Following the same working model, we could speculate that HPV49 E6 and E7, but not HPV38 E6 and E7, are able to efficiently neutralize the cellular defenses in the epithelial cells of the upper digestive tract activated by 4NQO.

In conclusion, our data highlight important differences in the biologic properties of certain beta HPV types, which may reflect their tissue tropism. The HPV phylogenetic tree has been generated considering differences in DNA sequence in the late gene *L1*, which is not necessarily linked to the biologic properties of the individual HPV types. Indeed, genus alpha includes low-risk and HR mucosal HPV types as well as benign cutaneous HPV types. Thus, it is not surprising that other genera, such as beta or gamma, could include HPV types with mucosal and cutaneous tropism.

Our studies in Tg mouse models also support the concept that these beta HPV types in the absence of any environmental factors are not pathogenic by themselves, as they do not induce any benign or malignant lesions spontaneously in experimental

genetic models. However, they considerably increase susceptibility to carcinogenesis by specific DNA damage agents.

These findings, if validated in other experimental models and studies, could lead to characterization of novel scenarios of virus-mediated carcinogenesis, facilitating the development of cancer preventive strategies.

## Disclosure of Potential Conflicts of Interest

No potential conflicts of interest were disclosed.

## Authors' Contributions

**Conception and design:** D. Viarisio, K. Müller-Decker, L. Gissmann, M. Tommasino

**Development of methodology:** D. Viarisio, M. Tommasino

**Acquisition of data (provided animals, acquired and managed patients, provided facilities, etc.):** D. Viarisio, K. Müller-Decker, P. Zanna, U. Kloz, B. Aengeneyndt, C. Flechtenmacher, M. Tommasino

**Analysis and interpretation of data (e.g., statistical analysis, biostatistics, computational analysis):** D. Viarisio, P. Zanna, C. Flechtenmacher, L. Gissmann, M. Tommasino

**Writing, review, and/or revision of the manuscript:** D. Viarisio, K. Müller-Decker, R. Accardi, C. Flechtenmacher, L. Gissmann, M. Tommasino

**Administrative, technical, or material support (i.e., reporting or organizing data, constructing databases):** D. Viarisio

**Study supervision:** D. Viarisio, M. Tommasino

## Acknowledgments

The authors thank all members of our laboratories at DKFZ and IARC for their cooperation, Dr. Katia Zanier for the analyses of the E6 structures, Nicole Suty for her help with preparation, and Dr. Karen Müller for editing this manuscript.

## Grant Support

The study was supported by a grant from Deutsche Krebshilfe (no. 110259 to L. Gissmann and M. Tommasino) and by a grant from "Fondation ARC" (no. PJA 20151203192 to M. Tommasino).

The costs of publication of this article were defrayed in part by the payment of page charges. This article must therefore be hereby marked *advertisement* in accordance with 18 U.S.C. Section 1734 solely to indicate this fact.

Received February 9, 2016; revised April 22, 2016; accepted May 4, 2016; published OnlineFirst May 23, 2016.

## References

1. Van Doorslaer K, Tan Q, Xirasagar S, Bandaru S, Gopalan V, Mohamoud Y, et al. The Papillomavirus Episteme: a central resource for papillomavirus sequence data and analysis. Nucleic Acids Res 2013;41:D571–8.
2. Tommasino M.The human papillomavirus family and its role in carcinogenesis. Semin Cancer Biol 2014;26:13–21.
3. Howley PM, Pfister HJ. Beta genus papillomaviruses and skin cancer. Virology 2015;479–480:290–6.
4. Bottalico D, Chen Z, Dunne A, Ostoloza J, McKinney S, Sun C, et al. The oral cavity contains abundant known and novel human papillomaviruses from the Betapapillomavirus and Gammapapillomavirus genera. J Infect Dis 2011;204:787–92.
5. Pierce Campbell CM, Messina JL, Stoler MH, Jukic DM, Tommasino M, Gheit T, et al. Cutaneous human papillomavirus types detected on the surface of male external genital lesions: a case series within the HPV Infection in Men Study. J Clin Virol 2013;58:652–9.
6. Torres M, Gheit T, McKay-Chopin S, Rodriguez C, Romero JD, Filotico R, et al. Prevalence of beta and gamma human papillomaviruses in the anal canal of men who have sex with men is influenced by HIV status. J Clin Virol 2015;67:47–51.
7. Forslund O, Johansson H, Madsen KG, Kofoed K. The nasal mucosa contains a large spectrum of human papillomavirus types from the Betapapillomavirus and Gammapapillomavirus genera. J Infect Dis 2013;208:1335–41.
8. Cornet I, Bouvard V, Campo MS, Thomas M, Banks L, Gissmann L, et al. Comparative analysis of transforming properties of E6 and E7 from different beta human papillomavirus types. J Virol 2012;86:2366–70.
9. Fuchs E.Keratins and the skin. Annu Rev Cell Dev Biol 1995;11:123–53.
10. Viarisio D, Mueller-Decker K, Kloz U, Aengeneyndt B, Kopp-Schneider A, Grone HJ, et al. E6 and E7 from beta HPV38 cooperate with ultraviolet light in the development of actinic keratosis-like lesions and squamous cell carcinoma in mice. PLoS Pathog 2011;7:e1002125.
11. United States Health Research Extension Act of 1985, Pub. L. No. 99–158, 99 Stat. 820 (Nov 20, 1985).
12. The Council of The European Communities. Council directive 86/609/EEC of 24 November 1986; 1986. Available from: http://ec.europa.eu/food/fs/aw/aw_legislation/scientific/86-609-eec_en.pdf.
13. Kallio MA, Tuimala JT, Hupponen T, Klemela P, Gentile M, Scheinin I, et al. Chipster: user-friendly analysis software for microarray and other high-throughput data. BMC Genomics 2011;12:507.
14. Huang da W, Sherman BT, Lempicki RA. Systematic and integrative analysis of large gene lists using DAVID bioinformatics resources. Nat Protoc 2009;4:44–57.
15. Huang da W, Sherman BT, Lempicki RA. Bioinformatics enrichment tools: paths toward the comprehensive functional analysis of large gene lists. Nucleic Acids Res 2009;37:1–13.
16. Strati K, Pitot HC, Lambert PF. Identification of biomarkers that distinguish human papillomavirus (HPV)-positive versus HPV-negative head and neck cancers in a mouse model. Proc Natl Acad Sci U S A 2006;103:14152–7.
17. Venkat JA, Shami S, Davis K, Nayak M, Plimmer JR, Pfeil R, et al. Relative genotoxic activities of pesticides evaluated by a modified SOS microplate assay. Environ Mol Mutagen 1995;25:67–76.
18. Ramotar D, Belanger E, Brodeur I, Masson JY, Drobetsky EA. A yeast homologue of the human phosphotyrosyl phosphatase activator PTPA is implicated in protection against oxidative DNA damage induced by the model carcinogen 4-nitroquinoline 1-oxide. J Biol Chem 1998;273:21489–96.
19. Kranendonk M, Pintado F, Mesquita P, Laires A, Vermeulen NP, Rueff J. MX100, a new Escherichia coli tester strain for use in genotoxicity studies. Mutagenesis 1996;11:327–33.
20. Panigrahi GB, Walker IG. The N2-guanine adduct but not the C8-guanine or N6-adenine adducts formed by 4-nitroquinoline 1-oxide blocks the 3′-5′ exonuclease action of T4 DNA polymerase. Biochemistry 1990;29:2122–6.
21. Thomas DC, Husain I, Chaney SG, Panigrahi GB, Walker IG. Sequence effect on incision by (A)BC excinuclease of 4NQO adducts and UV photoproducts. Nucleic Acids Res 1991;19:365–70.
22. Quint KD, Genders RE, de Koning MN, Borgogna C, Gariglio M, Bouwes Bavinck JN, et al. Human Beta-papillomavirus infection and keratinocyte carcinomas. J Pathol 2015;235:342–54.
23. Paolini F, Rizzo C, Sperduti I, Pichi B, Mafera B, Rahimi SS, et al. Both mucosal and cutaneous papillomaviruses are in the oral cavity but only alpha genus seems to be associated with cancer. J Clin Virol 2013;56:72–6.
24. Forslund O, Holmquist Mengelbier L, Gisselsson D. Regarding human cytomegalovirus in neuroblastoma. Cancer Med 2014;3:1038–40.
25. Zanier K, Charbonnier S, Sidi AO, McEwen AG, Ferrario MG, Poussin-Courmontagne P, et al. Structural basis for hijacking of cellular LxxLL motifs by papillomavirus E6 oncoproteins. Science 2013;339:694–8.
26. Martinez-Zapien D, Ruiz FX, Poirson J, Mitschler A, Ramirez J, Forster A, et al. Structure of the E6/E6AP/p53 complex required for HPV-mediated degradation of p53. Nature 2016;529:541–5.

27. Tang XH, Knudsen B, Bemis D, Tickoo S, Gudas LJ. Oral cavity and esophageal carcinogenesis modeled in carcinogen-treated mice. Clin Cancer Res 2004;10:301–13.
28. Giampieri S, Storey A. Repair of UV-induced thymine dimers is compromised in cells expressing the E6 protein from human papillomaviruses types 5 and 18. Br J Cancer 2004;90:2203–9.
29. Hufbauer M, Cooke J, van der Horst GT, Pfister H, Storey A, Akgul B. Human papillomavirus mediated inhibition of DNA damage sensing and repair drives skin carcinogenesis. Mol Cancer 2015; 14:183.
30. Schwarz A, Maeda A, Stander S, van Steeg H, Schwarz T. IL-18 reduces ultraviolet radiation-induced DNA damage and thereby affects photoimmunosuppression. J Immunol 2006;176: 2896–901.
31. Schwarz T, Schwarz A. DNA repair and cytokine responses. J Investig Dermatol Symp Proc 2009;14:63–6.